

Static Analysis of Cutting Tool using Finite Element Approach

Raju Sahu¹, Prateek Singh²

¹M.tech Scholar, Dept. of Mechanical Engineering,SSIPMT Raipur, Chhattisgarh, India

²Assistant Professor, Dept. of Mechanical Engineering,SSIPMT Raipur, Chhattisgarh, India

Abstract - In the field of production specifically in machining process cutting tool plays a very significant role. It not facilitates cutting task but also helps in acquiring perfect surface finish along with certain acceptable range of accuracy. To accomplish these, the tool has to be strong enough so that it can bear various continuous as well as repeatable load and it should have to wear resistant. In this paper a single point cutting tool has been examined with the help of finite element tool. A CAD model of single point cutting tool with work piece has been developed and to simulate adequate boundary conditions has been applied. Where total deformation and Von mises stress has been calculated for parametric various in tool signature.

Key Words: Cutting tool, FEA, Deformation, Stress, Rack angle.

1. INTRODUCTION

Design and manufacturing of cutting tools conquers a vital role in somewhat manufacturing scheme, as machining processes endure to grasp a large share of product shape and form realization activities. The computational modelling of any cutting tool commences with the modelling of a single point cutting tool. Conservatively, cutting tools have been stated using the principles of projective geometry and the classifications have been inadequate to few standard shapes of the cutting tools. They are not integrated and have a very narrow usage in computer aided manufacturing and engineering exploration. With more and more complex tools in practice, which result in increase in demand of customization of cutting tools in order to advance the cutting performance, there is a need to develop a computational analysis of cutting tools which can be directly used by computer controlled grinding machines for shape generation. A standard SPCT can be created through grinding or milling. If the tool is to be created through milling, generating the point cloud data for the surface is sufficient. But surfaces produced by milling do not give a good surface finish and some post processing is required. If the tool can be produced through grinding, the desired surface finish and accuracy are easier to achieve. But, to relate the geometric definition of the tool to grinding parameters, a detailed computational analysis of the tool signature in terms of deformation parameters is required.

2. LITERATURE REVIEW

(Sambhav et al. [1] followed the CAD approach to directly represent the sectional and point profile of the generic definition of a drill using NURBS in terms of the grinding parameters. But a detailed geometric model to represent a

generalized model of a SPCT to facilitate the grinding process needs to be worked out which is presented in this paper.

Deo [2] and Rajpathak [3] developed the geometry of single point cutting tools in terms of bi-parametric surface patches which was extended to multipoint cutting tools by Tandon et al. [4] to establish a set of new three-dimensional (3D) standards for defining the cutting tool geometries. They also established the forward and inverse mapping relations between 3D nomenclature and conventional specification schemes

Sambhav et al. [5] presented a generic mathematical model of single point cutting tools in terms of grinding angles where the angles and grinding depths could be varied continuously to obtain sculptured tool surfaces. They also verified the CAD definitions for the arbitrarily shaped cutting tools by comparing the points on the cutting edges obtained analytically with the rendered model. The forward and inverse mappings between the 3D nomenclature and conventional specification schemes were also explored for the generic SPCT

Hsieh [6] has presented the interrelationships among the tool angles, setting angles and working angles of a SPCT with the methodology to derive one set of angles from the other two sets.

Stephenson and Agapiou [7] described parametrically complex point geometries of a drill but they were not related to the grinding parameters.

Zhongqing [8] has brought out the shortcomings of a 2D representation of a cutter and modeled a 3D cutter using vector representation and presented the model of a turning cutter as an example.

Zhu et al. [9] have presented mechanistic models for different kinds of milling operations. Kang et al. [10] have used mechanistic model for micro end milling while Bhattacharya et al. [11] have accomplished the model for predicting the cutting force for arbitrary reamer geometry.

Experimentally, it was found by Wang et al. [12] that at 0° orientation, the main cutting force decreased with increased rake angle, whereas at positive orientations, increased rake angle caused increase in the thrust force. The optimum rake angle that would minimize the principle cutting force was found to be 30°.

Palanikumar [13] studied surface roughness when turning GFRP and found that it increases with increased fibre orientation and feed rate while it decreases with increased cutting speed and depth of cut.

Kim et al. [14] studied the effect of the edge radius for a cemented carbide tool on the cutting forces and temperature, using an FE orthogonal cutting model based on the Eulerian formulation, and compared the results with the experiments.

Their simulation results showed that increased tool edge radius alters the temperature distribution of the tool and shifts the position of maximum temperature closer to the tool tip. Experimental results also indicated that cutting forces increase as the tool edge radius increases.

Shintani et al. [15,16] analyzed the effect of tool geometry on the cutting performance of CBN tools for carburized hardened steel (600–720 HV) under both continuous and interrupted cutting conditions. Based on experimental results, covering an extensive range of tool geometric parameters, the optimum tool geometry for continuous cutting was specified to have a negative chamfer angle of 35°, a chamfer width larger than the tool–chip contact length (0.2 mm), a nose radius of 0.8 mm, and a hone radius of 0.05 mm.

Matsumoto et al. [17] investigated four different tool edge designs (sharp, honed, single chamfered and double chamfered) on residual stress in bar turning. They concluded that with the honed and double chamfered tools, the residual stress on the machined surface became more compressive and the affected zone reached a deeper sublayer.

Ren and Altintas [18] proposed an analytical cutting model for chamfer tools, based on Oxley’s slip-line field model [19] for sharp tools. They proposed to minimize the cutting energies in the deformation zones by analyzing the influence of chamfer angle and cutting conditions on the cutting forces and temperature.

3. METHODOLOGY

The equation of motion of cutting tool is solved using FEA tool (ANSYS) as the equation of motion for a cutting tool is difficult to visualize therefore some FEM tool is the solution method for analyzing stress of cutting tool with various aspect ratio.

The ANSYS 15 finite element program was used for stress analysis. For this purpose, the key points were first created and then line segments were formed. The lines were combined to create an area. Finally, this area was extruded. We modelled the cutting tool with a different tool signature. A three-dimensional structural solid element was selected to model the cutting tool. The cutting tool was discretized into 8811 elements with 10710. The cutting tool boundary conditions can also be modelled by constraining all degrees of freedoms of the nodes located on the left end of the cutting tool. For bending and contact stress analysis the cutting tool with the properties given in table 1 was chosen to model. To minimize computation time, meshed gear with one tooth is imported to ANSYS Workbench 15 for analysis)

Table 1: Cutting tool parameters

Material	Uncoated cemented carbide
Young’s modulus (GPa)	534
Poisson’s ratio	0.22
Density (kg/m ³)	11900
Thermal conductivity (W/m °C)	35.95 + 0.042T
Specific heat (J/kg °C)	334.01 + 0.12T

4. MATHEMATICAL MODELLING

The geometry of the problem herein investigated is depicted in Fig. 1.

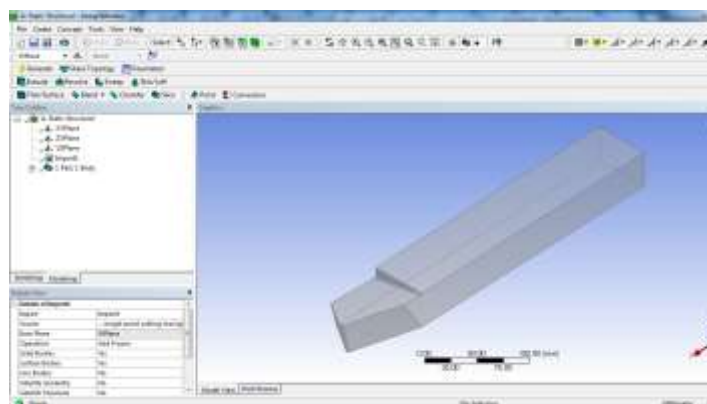


Fig. 1 Cutting tool

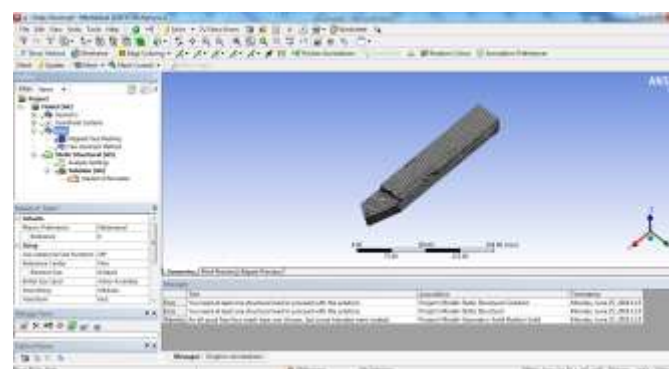


Fig. 2 Mesh Model

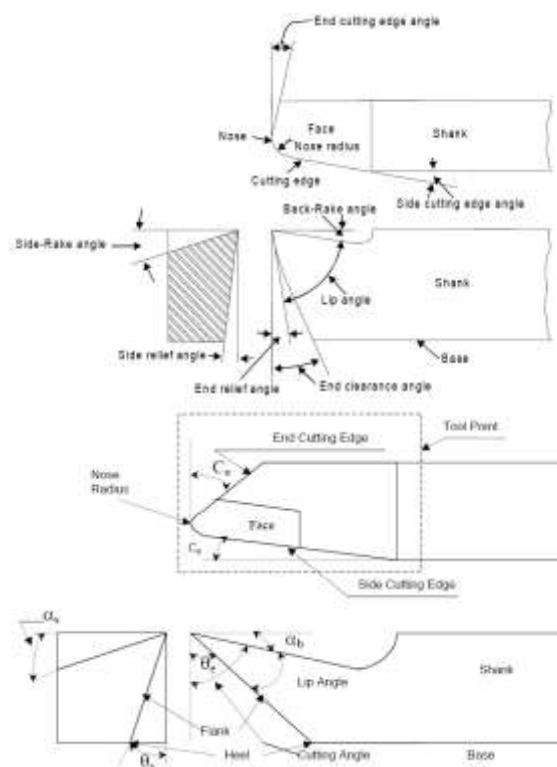


Fig 3 Tool parameters and signature

The FEM Formulation

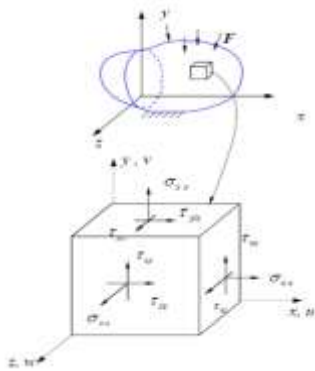


Figure 4 Infinitesimal element showing stress state [17].
Displacement

$$U = \{u(x, y, z), v(x, y, z), w(x, y, z)\}$$

Cauchy's Stress tensor =

$$\sigma = \begin{bmatrix} \sigma_{xx} & \tau_{xy} & \tau_{xz} \\ \tau_{yx} & \sigma_{yy} & \tau_{yz} \\ \tau_{zx} & \tau_{zy} & \sigma_{zz} \end{bmatrix}$$

The strain-stress relations (Hooke's law) for isotropic materials are given by:

$$\begin{Bmatrix} \epsilon_{xx} \\ \epsilon_{yy} \\ \epsilon_{zz} \\ \gamma_{xy} \\ \gamma_{yz} \\ \gamma_{xz} \end{Bmatrix} = \frac{1}{E} \begin{bmatrix} 1 & -\nu & -\nu & 0 & 0 & 0 \\ -\nu & 1 & -\nu & 0 & 0 & 0 \\ -\nu & -\nu & 1 & 0 & 0 & 0 \\ 0 & 0 & 0 & 2(1+\nu) & 0 & 0 \\ 0 & 0 & 0 & 0 & 2(1+\nu) & 0 \\ 0 & 0 & 0 & 0 & 0 & 2(1+\nu) \end{bmatrix} \begin{Bmatrix} \sigma_{xx} \\ \sigma_{yy} \\ \sigma_{zz} \\ \tau_{xy} \\ \tau_{yz} \\ \tau_{zx} \end{Bmatrix}$$

Strain-Displacement relations are:

$$\epsilon_{xx} = \frac{\partial u}{\partial x}, \epsilon_{yy} = \frac{\partial v}{\partial y}, \epsilon_{zz} = \frac{\partial w}{\partial z}, \gamma_{xy} = \frac{\partial v}{\partial x} + \frac{\partial u}{\partial y},$$

$$\gamma_{yz} = \frac{\partial w}{\partial y} + \frac{\partial v}{\partial z}, \gamma_{xz} = \frac{\partial u}{\partial z} + \frac{\partial w}{\partial x}$$

$$\frac{\partial \sigma_{xx}}{\partial x} + \frac{\partial \tau_{xy}}{\partial y} + \frac{\partial \tau_{xz}}{\partial z} + X = 0$$

$$\frac{\partial \tau_{xy}}{\partial x} + \frac{\partial \sigma_{yy}}{\partial y} + \frac{\partial \tau_{yz}}{\partial z} + Y = 0$$

$$\frac{\partial \tau_{xz}}{\partial x} + \frac{\partial \tau_{yz}}{\partial y} + \frac{\partial \sigma_{zz}}{\partial z} + Z = 0$$

$$(\lambda + G) \frac{\partial e}{\partial x} + G \nabla^2 u + X = 0$$

$$e = \epsilon_{xx} + \epsilon_{yy} + \epsilon_{zz} = \frac{\partial u}{\partial x} + \frac{\partial v}{\partial y} + \frac{\partial w}{\partial z}$$

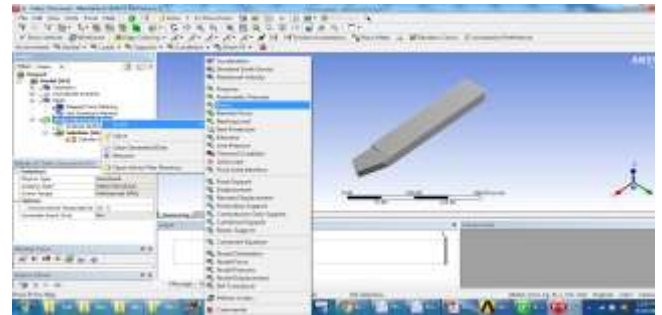


Fig. 5 ANSYS Workbench force selection

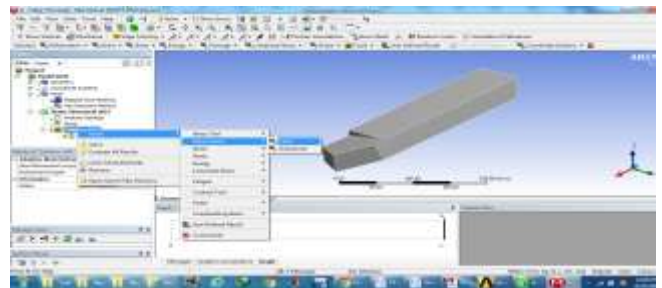


Fig. 6 ANSYS Workbench solution preference total deformation

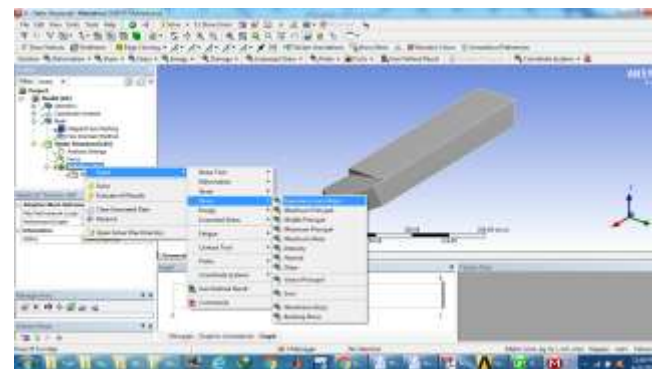


Fig. 7 ANSYS Workbench solution preference equivalent Von Mises Stress

5. Result and Discussion

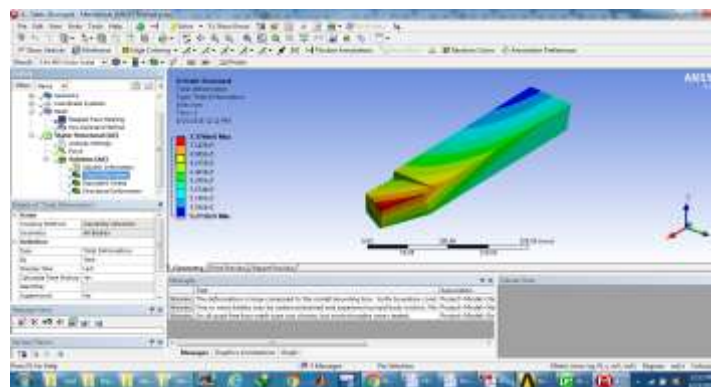


Figure 8 ANSYS Workbench result

Figure 9 shows that the effect of relief angle on the cutting tool. It has been observed that an increase in relief angle the Von Mises stress decreases significantly. The main role of relief angle is that it prevents rubbing action below cutting edge. Small relief angle gives maximum support below the cutting edge and is necessary while machining hard and strong workpiece. Too much relief angle weakens the cutting edge and failure of the tool may take place.

Fig 10 and 11 shown the effect of a back rake angle on the cutting tool. It has been observed that an increase in back rake angle decreases the tool stress level significantly. It has also been seen that the cutting force decreases with an increase in back rake angle. Positive back rake angle helps in moving chips away from the machined workpiece as the tool easily penetrates the workpiece and leads to shearing of material rather than compressing, which ultimately improves the cutting efficiency. The same can be evident from the figure 12.

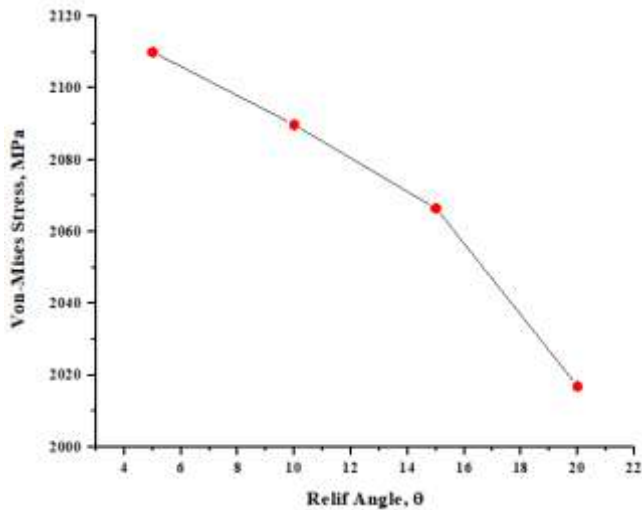


Fig. 9 Effect of Relief angle of Von-Mises Stress

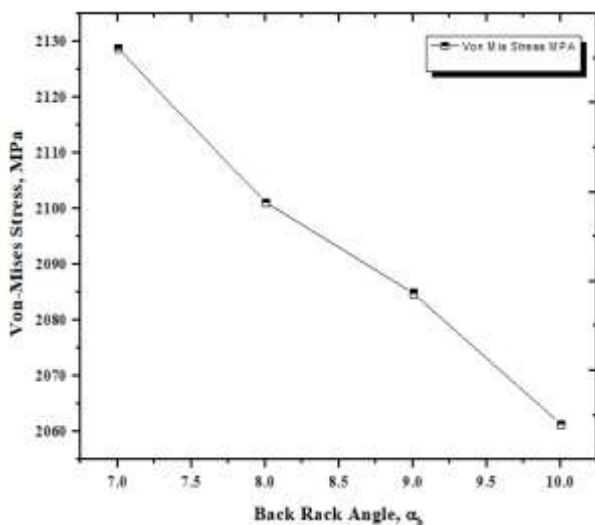


Fig. 10 Effect of Back Rake angle on Von-Mises Stress

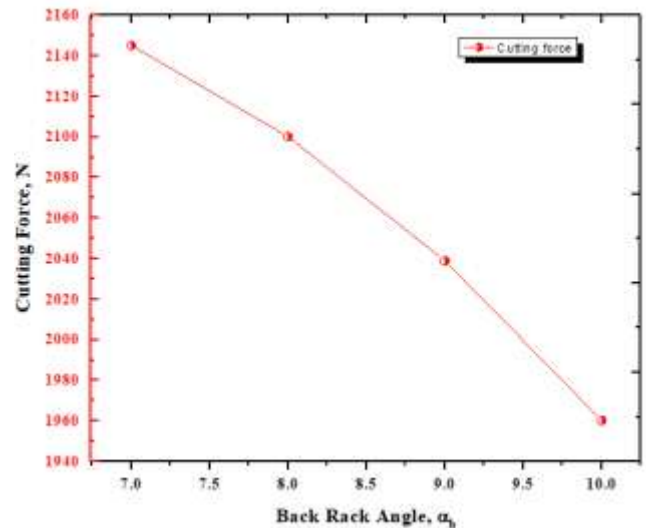


Fig. 11 Effect of Back Rake angle on Von-Mises Stress

From the above, it can be concluded that for cutting harder material positive rake angle is preferred. The chip from the workpiece moves away from the tool due to positive rake angle. Therefore, low tensile strength, as well as non ferrous materials are machined by using a positive rake angle. However, a positive rake angle based tool has also been used for machining long and small diameter shafts or material that is work hardened during machining. Even from the figure 12, we can conclude that during machining hardened material continuous chip is generated which is desirable in order to maintain the cutting tool under the safer zone and prevents it from failure. Thus it can be proved that for cutting hardened material positive rake angle is used which results in the generation of continuous chip and prevent the cutting tool from failure.

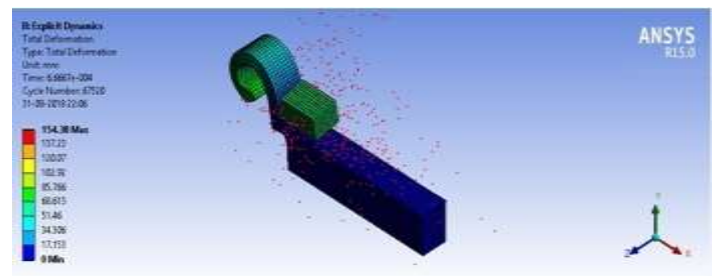


Fig. 12 Total Deformation of the Cutting tool

6. CONCLUSION

on the basis of finite element analysis following conclusion has been drawn which are as follows:

- Increase in back rake angle decreases the tool stress level and cutting force.
- Positive back rake angle helps in moving chips away from the cutting tool and work piece.
- Positive back rake angle is widely being used in machining low tensile strength material and non ferrous material.

- Increase in relief angle, decreases Von-Mises stress. For machining harder material small relief angle is preferred larger relief angle leads to deterioration of cutting edge and the cutting tool ultimately fails.
- Increase in back rake angle the cutting force eventually decreases.

REFERENCES

- [1] K. Sambhav, S.G. Dhande, P. Tandon, CAD based mechanistic modeling of forces for generic drill point geometry, *Comput. Aided Design Appl.* 7 (6) (2010) 809–819
- [2] Y.V. Deo, Geometric Modeling of Single Point and Fluted Tool Surfaces, M.Tech. Thesis, IIT Kanpur, 1997
- [3] T.S. Rajpathak, Geometric modeling of single point cutting tools for grinding and sharpening, M.Tech. Thesis, IIT Kanpur, 1996
- [4] P. Tandon, P. Gupta, S.G. Dhande, Geometric modeling of single point cutting tool surfaces, *Int. J. Adv. Manuf. Technol.* 22 (2003) 101–111.
- [5] K. Sambhav, P. Tandon, S.G. Dhande, A generic mathematical model of single point cutting tools in terms of grinding parameters, *Applied Mathematical Modelling* 35 (10) (2011) 5143–5164
- [6] J.F. Hsieh, Mathematical modeling of interrelationships among cutting angles, setting angles and working angles of single-point cutting tools, *Appl. Math. Model.* 34 (2010) 2738–2748.
- [7] D.A. Stephenson, J.S. Agapiou, Calculation of main cutting edge forces and torque for drills with arbitrary point geometries, *Int. J. Mach. Tools Manuf.* 32 (1992) 521–538
- [8] W. Zhongqing, Research on forming theory of a 3D body by the constructing cutting geometry method (CCG), *J. Mater. Process. Technol.* 139 (2003) 539–542
- [9] R. Zhu, S.G. Kapoor, R.E. DeVor, Mechanistic modeling of the ball end milling process for multi-axis machining of free-form surfaces, *ASME Journal of Manufacturing Science and Engineering* 123 (2001) 369–379.
- [10] I.S. Kang, J.S. Kim, M.C. Kang, Y.W. Seo, A mechanistic model of cutting force in micro end milling process, *Journal of Materials Processing Technology* 187–188 (2007) 250–255
- [11] O. Bhattacharya, S.G. Kapoor, R.E. Devor, Mechanistic model for the reaming process with emphasis on process faults, *International Journal of Machine Tools & Manufacture* 46 (2006) 836–846
- [12] D. H. Wang, M. Ramulu, D. Arola, Orthogonal cutting mechanisms of graphite/epoxy composite. Part I: unidirectional laminate, *Int. J. of Machine Tools and Manufacture* 35 (1995) 1623–1638.
- [13] K. Palanikumar, Modeling and analysis for surface roughness in machining glass fibre reinforced plastics using response surface methodology, *Materials & Design* 28 (2007) 2611–2618
- [14] K.W. Kim, W.Y. Lee, H.C. Sin, A finite-element analysis of machining with the tool edge considered, *J. Mater. Process. Technol.* 86 (1999) 45–55
- [15] K. Shintani, M. Ueki, Y. Fujimura, Optimum tool geometry of CBN tool for continuous turning of carburized steel, *Int. J. Mach. Tools Manuf.* 26 (3) (1989) 403–413.
- [16] K. Shintani, M. Ueki, Y. Fujimura, Optimum cutting tool geometry when interrupted cutting carburized steel by CBN tool, *Int. J. Mach. Tools Manuf.* 26 (3) (1989) 415–423.
- [17] Y. Matsumoto, F. Hashimoto, G. Lahoti, Surface integrity generated by precision hard turning, *Ann. CIRP* 48 (1) (1999) 59–62.
- [18] H. Ren, Y. Altintas, Mechanics of machining with chamfered tools, *Trans. ASME J. Manuf. Sci. Eng.* 122 (2000) 650–659.
- [19] P.L.B. Oxley, *Mechanics of Machining—An Analytical Approach to Assessing Machinability*, Ellis Horwood, Chichester, UK, 1989.